

Parametric Study and Design of Implantable PIFAs for Wireless Biotelemetry

Asimina Kiourti, Michalis Tsakalakis, and Konstantina S. Nikita

National Technical University of Athens, School of Electrical and Computer Engineering
akiourti@biosim.ntua.gr, knikita@ece.ntua.gr

Abstract. The design parameters of a skin–implantable planar inverted–F antenna (PIFA) operating in the 402–405 MHz Medical Implant Communications Service (MICS) band are studied and their impact on the exhibited resonance characteristics is assessed. Based on the parametric results, two novel MICS PIFAs are proposed for skin–implantation. The study, thus, evaluates the tuning stability of a novel implantable PIFA on potential manufacturing inaccuracies. Significant guidance on implantable PIFA design is also provided. Numerical results based on Finite Element Method (FEM) numerical simulations are presented.

Keywords: Finite element method (FEM), implantable antenna, medical implant communications service (MICS) band, parametric study.

1 Introduction

Significant research is, nowadays, carried out on the design of medical implant–integrated antennas for biomedical telemetry in the Medical Implant Communications Service (MICS) frequency band (402–405 MHz) which is regulated by the Federal Communications Commission (FCC) [1] and the European Radiocommunications Committee (ERC) [2] for ultra–low–power active medical implants [3]–[9]. Stacked planar inverted–F antennas (PIFAs) are most commonly preferred because of their flexibility in size miniaturization, bandwidth enhancement, biocompatibility and conformability [5]–[9].

In this study, we evaluate the detuning caused by manufacturing inaccuracies in a stacked alumina 96%–PIFA with meandered patches, operating in the MICS band while implanted in skin tissue. Position of the shorting pin, meanders’ lengths and widths, and dielectric thickness and material are parametrically studied to assess their impact on the antenna resonance frequency and its ability to operate in the MICS band. Significant guidance on implantable PIFA design is also provided. Based on the initial PIFA configuration and the derived parametric results, two novel skin–implantable Rogers 3210–PIFAs are proposed for biotelemetry in the MICS band. Finite Element Method (FEM) numerical simulations are performed [10].

The rest of the paper is organized as follows. In Section 2, a skin–implantable miniature alumina 96%–PIFA is proposed and parametrically studied. In Section 3,

two novel skin–implantable Rogers 3210–PIFAs are designed based on the derived parametric results. The paper concludes in Section 4.

2 Parametric Study

The parametric PIFA model of Fig. 1(a)–(d) is considered [8], [9]. The PIFA consists of an R -radius ground plane and two R_p -radius vertically-stacked meandered patches, printed on h_1 - and h_2 -thick dielectric substrates, respectively. Meanders are equi-distant (d), have the same width (w), and their lengths are denoted by l_i , where i is the meander number (Fig. 1(b), (c)). Patches are fed by a 50 Ohm-coaxial cable centered at F (0 mm, 3 mm) and radiate, while a 0.2 mm-radius shorting pin connects the ground plane with the lower patch at S (s_x, s_y). An h_3 -thick dielectric superstrate covers the structure to preserve its biocompatibility and robustness.

Since the PIFA is intended for skin tissue implantation, the simulation setup of Fig. 2 is considered, in which the antenna is assumed to be implanted in the center of a 100 mm–edge skin tissue simulating cube ($\epsilon_r = 46.7$, $\sigma = 0.69$ S/m at 402 MHz [11]) [8], [9]. Iterative simulation tests are performed, and the variable values of Table 1 and 2 (PIFA I) are finally found to tune PIFA I at the desired frequency of 402 MHz (Fig. 3(a)), as demonstrated by the authors in [8].

Slight deviations around the original variable values of PIFA I are considered hereafter, and their effects on the exhibited resonance characteristics are discussed. Finite element (FE) simulations are conducted in which automatic iterative tetrahedron–meshing refinement is performed. Iterative refinement stops when the change in the magnitude of the reflection coefficient (in absolute value) between two consecutive passes is less than 0.02. Free–space surrounds the simulation setup of Fig. 2 by 200 mm ($\lambda_0/4 \approx 186.5$ mm, where λ_0 is the free–space wavelength at 402 MHz), while radiation boundaries extend radiation infinitely far into space.

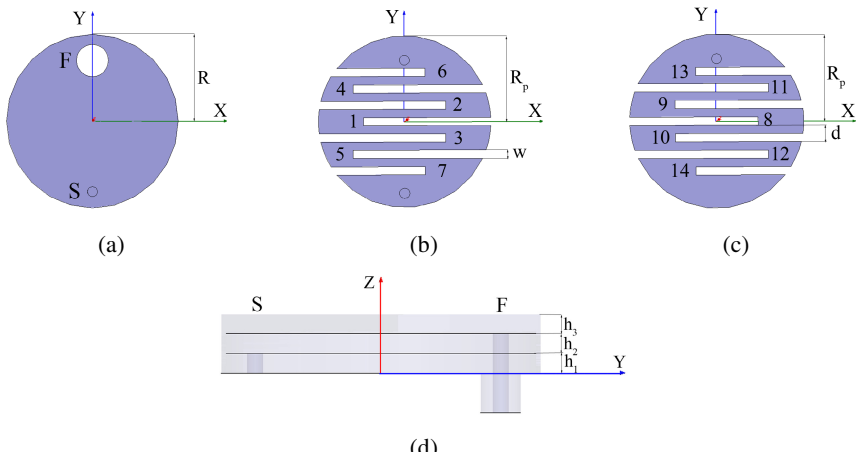


Fig. 1. Configuration of the proposed parametric PIFA model: (a) ground plane, (b) lower patch, (c) upper patch, and (d) side view

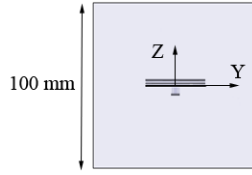


Fig. 2. Simulation set-up: PIFA implanted in the center of a 100 mm–edge skin tissue cube [8], [9]

Table 1. Meanders' lengths (Fig. 1) for PIFA I, PIFA II and PIFA III (in [mm])

	l_1	$l_2 = l_3$	$l_4 = l_5$	$l_6 = l_7$	l_8	$l_9 = l_{10}$	$l_{11} = l_{12}$	$l_{13} = l_{14}$
PIFA I (alumina 96%)	7.4	5.8	4.5	0	7.4	5.8	4.5	0
PIFA II (Rogers 3210)	7.2	6.5	5.2	0	8.3	7.9	7.3	0
PIFA III (Rogers 3210)	4.9	5.1	6.4	5.9	7.9	7.8	6.6	5.8

Table 2. Design variable values (Fig. 1) for PIFA I, PIFA II and PIFA III (in [mm])

	R	R_p	$h_1 = h_2$	h_3	d	w	s_x	s_y
PIFA I (alumina 96%)	4	3.9	0.25	0.15	1	0.5	3	-1
PIFA II (Rogers 3210)	4.5	4.4	0.635	0.635	1	0.5	0.3	-3.2
PIFA III (Rogers 3210)	4.3	4.2	0.635	0.635	0.7	0.35	0	-3

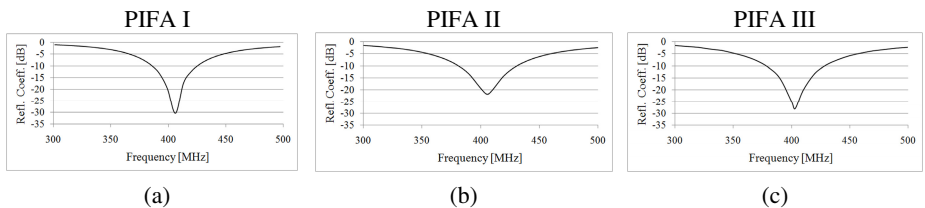


Fig. 3. Reflection coefficient frequency responses of (a) PIFA I, (b) PIFA II, and (c) PIFA III

2.1 Effect of Shorting Pin Position

Shorting the PIFA ground plane with the lower patch increases its effective size in a way which strongly depends on the exact position of the shorting pin. The design can be thought of as a modified monopole, since the shorting pin acts in much the same way as a ground plane on a monopole antenna, enhancing its electrical size. The further the shorting pin is placed on the “serpentine” current flow path which starts

from the PIFA feed point (F), the more the effective size of the PIFA is enhanced, and, thus, the lower its resonance frequency becomes (Fig. 4(a)), where positioning of the shorting pin at the end of meanders 1 to 5 is examined.

The values of the reflection coefficient achieved at the desired operation frequency of 402 MHz ($|S_{11}|_{@402\text{MHz}}$) are shown in Fig. 4(b) for each of the simulation scenarios. Assuming that satisfactory operation of the PIFA in the MICS band is guaranteed when $|S_{11}|_{@402\text{MHz}} < -10$ dB, then PIFA I is found to appropriately operate only in the case where the shorting pin is re-positioned at the end of meander 5.

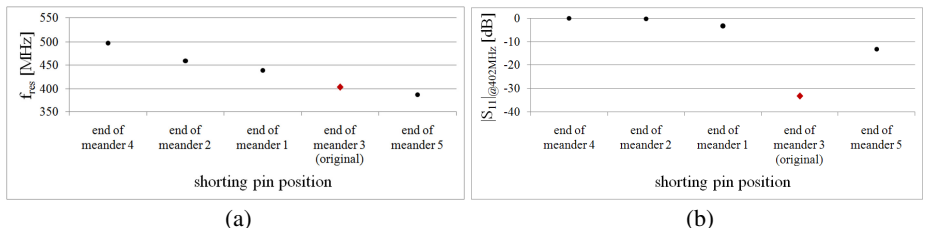


Fig. 4. Effect of shorting pin position on the (a) resonance frequency (f_{res}), and (b) reflection coefficient at 402 MHz ($|S_{11}|_{@402\text{MHz}}$) of PIFA I

2.2 Effect of Meanders' Length and Width

Longer (wider) meanders increase the length of the “serpentine” current path on the radiating patches, or, equivalently, the effective size of the PIFA, thus decreasing its resonance frequency, as shown in Fig. 5(a) (Fig. 6(a)). As expected, more intense deviations are observed in PIFA resonance frequency when all meanders are simultaneously lengthened (widened), rather than when the meanders of only the lower or upper patch are modified.

Simultaneous change in all meanders' lengths and widths by around ± 0.2 mm (Fig. 5(b)) and ± 0.1 mm (Fig. 6(b)), respectively, is found to preserve adequate operation of the antenna in the MICS band. The aforementioned values increase to approximately ± 0.3 mm (Fig. 5(b)) and ± 0.2 mm (Fig. 6(b)), respectively, when the lengths and widths of only a single patch (either the lower or upper) are modified.

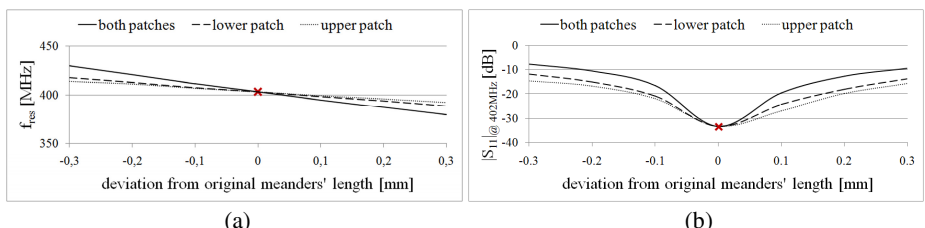


Fig. 5. Effect of meanders' length on the (a) resonance frequency (f_{res}), and (b) reflection coefficient at 402 MHz ($|S_{11}|_{@402\text{MHz}}$) of PIFA I

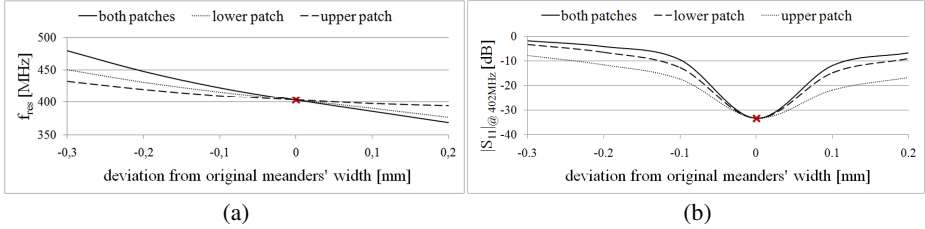


Fig. 6. Effect of meanders' width on the (a) resonance frequency (f_{res}), and (b) reflection coefficient at 402 MHz ($|S_{11}| @ 402 \text{ MHz}$) of PIFA I

2.3 Effect of Dielectric Thickness

Thicker dielectric layers isolate the PIFA from the high-dielectric constant skin tissue, thus decreasing its effective dielectric constant and electrical length, while increasing its resonance frequency. This phenomenon is apparent in Fig. 7(a) in the cases where changes in the upper substrate (h_2)– and superstrate (h_3)–thicknesses are considered. Modifying the lower substrate thickness (h_1) also affects the shorting pin-related resonance effect, overall resulting in lower resonance frequencies for higher values of h_1 .

As shown in Fig. 7(b), only slight deviations (of the order of less than ± 0.05 mm) from the original dielectric material thicknesses are allowed in order to preserve satisfactory operation of the PIFA in the MICS band.

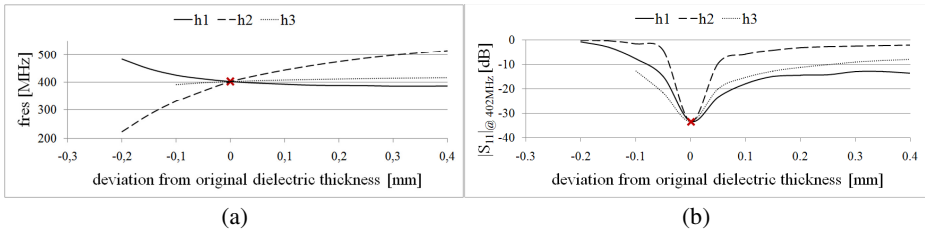


Fig. 7. Effect of dielectric thickness on the (a) resonance frequency (f_{res}), and (b) reflection coefficient at 402 MHz ($|S_{11}| @ 402 \text{ MHz}$) of PIFA I

2.4 Effect of Dielectric Material

Resonance frequencies achieved when substituting the dielectric material of PIFA I (alumina 96%, $\epsilon_r = 9.4$) with other dielectric materials commonly used in implantable antenna design (teflon ($\epsilon_r = 2.1$), macor ($\epsilon_r = 6.1$), alumina 92% ($\epsilon_r = 9.2$) and Rogers 3210 ($\epsilon_r = 10.2$) [5]–[9], [12]) are shown in Fig. 8(a). Higher dielectric constant–materials shorten the PIFA's wavelength, increase its electrical length and are, thus, found to decrease its resonance frequency.

Adequate performance of PIFA I in the MICS band is achieved only in the case where the dielectric is to be substituted with a material of highly similar dielectric constant, ϵ_r , such as alumina 92% (Fig. 8(b)). The choice of substrate and superstrate

materials is thus proved to be highly critical in the design and performance of miniature implantable PIFAs.

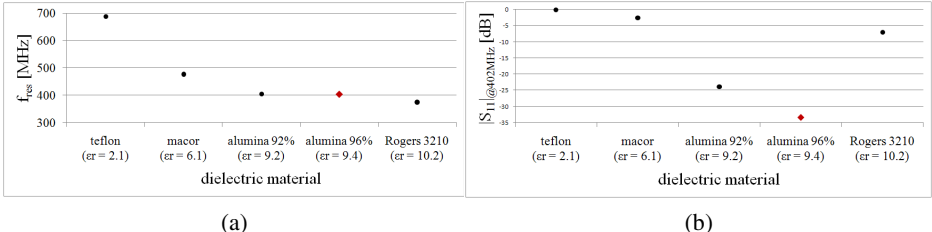


Fig. 8. Effect of dielectric material on the (a) resonance frequency (f_{res}), and (b) reflection coefficient at 402 MHz ($|S_{11}|_{@402 \text{ MHz}}$) of PIFA I

3 Design of Novel Implantable PIFAs

The parametric results of Section 2 provide significant guidance on the design of implantable PIFAs. For example, if the dielectric material of PIFA I is to be replaced with Rogers 3210 ($\epsilon_r = 10.2$, versus $\epsilon_r = 9.4$ for alumina 96%) [5]–[7], a decrease in resonance frequency is expected (Fig. 8(a)). However, the minimum available thickness of Rogers 3210–sheets (0.635 mm, versus 0.15 mm for alumina 96%) weakens tissue–loading on the PIFA, overall increasing its resonance frequency (Fig. 7(a)). PIFA design variables can, thus, be suitably selected (Table 1 and 2, PIFA II) to enhance its physical and/or effective size, and achieve an adequately low reflection coefficient at the desired operating frequency of 402 MHz (Fig. 3(b)).

Another example would be attempting to decrease the physical size (R) of PIFA II, while enhancing its effective size instead. Re–design consists of reducing the meanders’ width (w) and separation distance (d) to allow space for extra meanders, and adding two extra meanders to each of the patches. In this way, lengthening of the “serpentine” current path is achieved. Iterative tests can be performed to identify those variable values (Table 1 and 2, PIFA III) which achieve the desired resonance characteristics (Fig. 3(c)).

4 Conclusion

Design variables of a skin–implantable MICS PIFA were parametrically studied through FEM simulations to assess their impact on antenna resonance and the ability of the antenna to adequately operate in the MICS band (defined as $|S_{11}|_{@402 \text{ MHz}} < -10$ dB). Even minor deviations from the original parameter values were found to considerably alter the PIFA resonance frequency, and degrade its performance at the desired operating frequency of 402 MHz.

Significant guidance on implantable PIFA design was also provided. Based on the parametric results, two novel PIFAs were proposed for skin–implantation and wireless biotelemetry in the MICS band. Several other implantable PIFAs can be

designed to suit specific size constraints, material–availability limitations, bandwidth requirements and resonance detuning sensitivity values. Finally, the parametric results can be generalized to the design of PIFAs operating in other frequency bands and implanted in any type of human tissue.

References

1. Medical implant communications service (MICS) federal register. Rules Reg. 64, 69926–69934 (1999)
2. ERC recommendation 70–03 relating to the use of short range devices (SRD). Conf. Eur. Postal Telecomm. Admin (EPT), CEPT/ERC 70–03, Annex 12 (1997)
3. Sani, A., Alomainy, A., Hao, Y.: Numerical Characterization and Link Budget Evaluation of Wireless Implants Considering Different Digital Human Phantoms. *IEEE Transactions on Microwave Theory and Techniques* 57, 2605–2613 (2009)
4. Abadia, J., Merli, F., Zurcher, J.-F., Mosig, J.R., Skrivervik, A.K.: 3D-Spiral Antenna Design and Realization for Biomedical Telemetry in the MICS Band. *Radioengineering* 18, 359–367 (2009)
5. Liu, W.-C., Chen, S.-H., Wu, C.-M.: Bandwidth Enhancement and Size Reduction of an Implantable PIFA Antenna for Biotelemetry Devices. *Microwave and Optical Technology Letters* 51, 755–757 (2009)
6. Karacolak, T., Cooper, R., Topsakal, E.: Design of a Dual-Band Implantable Antenna and Development of Skin Mimicking Gels for Continuous Glucose Monitoring. *IEEE Transactions on Microwave Theory and Techniques* 56, 1001–1008 (2008)
7. Liu, W.-C., Chen, C.-H., Wu, C.-M.: Implantable Broadband Circular Stacked PIFA for Biotelemetry Communication. *Journal of Electromagnetic Waves and Applications* 22, 1791–1800 (2008)
8. Kiourti, A., Christopoulou, M., Nikita, K.S.: Performance of a Novel Miniature Antenna Implanted in the Human Head for Wireless Biotelemetry. In: 2011 IEEE International Symposium on Antennas and Propagation (2011)
9. Kiourti, A., Christopoulou, M., Koulouridis, S., Nikita, K.S.: Design of a novel miniaturized implantable PIFA for biomedical telemetry. In: Lin, J., Nikita, K.S. (eds.) *MobiHealth 2010. LNICST*, vol. 55, pp. 127–134. Springer, Heidelberg (2011)
10. Sadiku, M.N.O.: *Numerical Techniques in Electromagnetics*, 2nd edn. CRC Press (2001)
11. Gabriel, C., et al.: The Dielectric Properties of Biological Tissues. *Physics in Medicine and Biology* 41, 2231–2293 (1996)
12. Sootornpipit, P., Furse, C.M., Chung, Y.C.: Design of Implantable Microstrip Antenna for Communication with Medical Implants. *IEEE Transactions on Microwave Theory and Techniques* 52, 1944–1951 (2004)